Variations of the Somali upwelling since 18.5 ka BP and its relationship with southwest monsoon rainfall

Balaji D.[1,2], Ravi Bhushan[2], L. S. Chamyal[1]

[1]Department of Geology, The Maharaja Sayajirao University of Baroda, India
[2]Geoscience Division, Physical Research Laboratory, Ahmedabad, India

Correspondence to: Balaji D. (balaji.d86@gmail.com)

Abstract. Somali upwelling history has been reconstructed for the last 18.5 ka based on biogenic silica fluxes estimated from a sediment core retrieved from the western Arabian Sea. Surface winds along the east African coast during southwest monsoon causes the Somali upwelling and thus intensity of this upwelling has been related to the southwest monsoonal variability. Biogenic silica flux variation suggests periodic weakening and strengthening of the Somali upwelling. Weakened upwelling during 18.5-15 ka BP and strengthened upwelling during the Bølling-Allerød (15-12.9 ka BP) suggest onset of the southwest monsoon. Whereas the Younger Dryas (12.9-11.7 ka BP) is marked by reduced upwelling strength, intensification of the Somali upwelling occurred at the beginning of the Holocene and further declined at 8 ka BP. Increase in upwelling strength recorded since 8 ka BP suggest southwest monsoon strengthening during the latter part of the Holocene. Comparison of upwelling variations with the southwest monsoon precipitation record demonstrate a reversal in the relationship between the strength of the Somali upwelling and southwest monsoon rainfall at the beginning of the Holocene. The observed shift has been attributed to the variation in the southwest monsoon strength due to the latitudinal shift of the Intertropical Convergence Zone (ITCZ) associated with changes in moisture sources.

1 Introduction

A large fraction of the world's population resides in the tropical region, where climate is mainly driven by monsoon rainfall. Understanding the causes of past climatic changes thus plays a crucial role in deciphering past, present and future monsoon variability. India being a tropical country comprising significant fraction of the world's population, its economy is largely dependent on the southwest monsoon (SWM) rainfall; hence, slight changes in SWM rainfall can have immense societal impacts. Several attempts have been made to identify the factors responsible for SWM rainfall variations. SWM rainfall variability is correlated with several global phenomena, such as ENSO (Goswami et al., 1999; Annamalai and Liu, 2005), Atlantic Sea Surface Temperature (SST; Goswami et al., 2006; Yadav, 2016), Eurasian snow cover (Hahn and Shukla, 1976; Pant and Rupa Kumar, 1997; Bamzai and Shukla, 1999), the pre-monsoon 500 hPa ridge (Mooley et al., 1986), the Indo-Pacific warm pool (Parthasarathy et al., 1988; Parthasarathy et al., 1991), the Pacific decadal oscillation (Krishnan and Sugi, 2003), and the Atlantic multi-decadal oscillation (Krishnamurthy and Krishnamurthy, 2015). In addition to these factors that

influence SWM, the Indian Ocean Warm Pool (IOWP) has been identified as the prominent source of moisture for the SWM rainfall (Ninomiya and Kobayashi, 1999; Gimeno et al., 2010). During its maxima, the IOWP extends throughout the northern Indian Ocean during the pre-monsoon period (April), and it almost reduces to half during the SWM (Izumo et al., 2008). The extent of the IOWP is primarily controlled by the Somali upwelling and partly by the latent heat flux increase in the Arabian Sea during the SWM season (Izumo et al., 2008). Both Somali upwelling, as well as SWM rainfall, are triggered by the SWM winds during boreal summer.

Upwelling of deep water during the SWM brings nutrients to the photic zone, thereby enhancing surface productivity in the western Arabian Sea. Paleoproductivity variations in the coastal regions off Somalia and Oman have been extensively studied to understand past changes in SWM-related upwelling (Sirocko et al., 1993; Naidu and Malmgren, 1996; Gupta et al., 2003; Tiwari et al., 2010). Most of these previous studies were based on foraminifera shell abundance or its chemistry. The foraminifera production persists throughout the year in the study area with maximum production during monsoon seasons. Siliceous productivity in the study area being restricted to the southwest monsoon season can serve as a better proxy for upwelling. The variations in siliceous productivity in the western Arabian Sea thus have direct implication to the upwelling strength during the past. The siliceous productivity can be studied using the biogenic silica flux in the marine sediments.

The present study thus aims to understand past variations in siliceous productivity in the Somali upwelling region, as well as paleo-upwelling strength and its relationship with the southwest monsoon rainfall, using a sediment core retrieved from the western Arabian Sea (Fig. 2). The surface waters of the world ocean are mostly deficient in bioavailable silica (Hurd, 1973), which is a major nutrient for siliceous productivity. Apart from the Southern Ocean, high siliceous productivity can be observed in the major upwelling regions, where upwelled nutrient-rich water causes high primary production (Koning et al., 2001). The ocean is undersaturated with respect to silica, and thus biogenic silica flux in sediments is a function of its export flux, which is controlled by its production at the surface and dissolution in the water column as well at the sediment water interface (Hurd, 1989; Broecker and Peng, 1982). The use of biogenic silica as a proxy for the study of paleo-upwelling requires an understanding of its production and burial efficiency. Sediment trap studies from the western Arabian Sea indicated that biogenic silica flux mimics the SWM upwelling (Fig. 1; Nair, 2000; Haake et al., 1993). Studies of sediment trap data and surface sediments (Koning et al., 1997; Koning et al., 2001) of the Somali basin provide better estimates of the burial efficiency of biogenic silica i.e. ratio between diatom abundance at surface to its concentration in the sediment of the western Arabian Sea. Only 6.8–8.7 % of diatom (biogenic silica) productivity is preserved in the sediments of the Somali basin; the rest being remineralised in the water column and at the sediment water interface (Koning et al., 2001). One of the major findings by Koning et al., (2001) from sediment traps in the Somali basin is the selective preservation of upwelling-indicating diatoms in the sediments of the Somali region. This is linked to the silicification of diatom frustules; most pre- and post-upwelling produced diatoms are weakly silicified, enhancing their dissolution in the water column leading to their low preservation in sediments. Better preservation of upwelling indicating diatoms can also be linked to the increased downward supply due to high surface production. Nutrient availability (Si:N) and concentration of dissolved iron can affect diatom silicification that leads to variation in preservation (Hutchins and Bruland, 1998). In general, it is noted that high silicate concentration along

with micro-nutrient depletion leads to more silicified and faster sinking diatoms (Hutchins and Bruland, 1998), a most plausible scenario during the late phase of SWM upwelling. If burial efficiency (BE) is the primary controller of biogenic silica flux variation, ratio of low flux to low BE should have been similar to the ratio of high flux to high BE. However, in the present record using the modern high and low BE values (Koning et al., 2001), the ratio of high flux to high BE (sediment core top) is almost three times more than the ratio of low flux to low BE (sediment core bottom), thereby indicating the absence of preservation effect in the biogenic silica flux.

Apart from biogenic silica production and preservation efficiency, sediment redistribution can also influence the biogenic silica flux. However, considering the sediment core location and average sedimentation rate, it is likely that the influence of sediment focusing/winnowing on the flux record is minimal. The location of the sediment core is far from the continental slope (Fig. 2) and is not directly influenced by coastal currents or fluvial systems that would lead to redistribution of the sediment flux. The high surface production of biogenic silica during SWM upwelling (Fig. 1; Haake et al., 1993; Koning et al., 1997), together with the increased burial efficiency of upwelling-indicating diatoms (biogenic silica) in the western Arabian Sea sediments (Koning et al., 2001), makes biogenic silica flux, a potential proxy for SWM-related upwelling in the study area.

1.1Modern Oceanography and Productivity

The surface water circulation in the western Arabian Sea is controlled by seasonal changes in atmospheric wind pattern associated with annual migration of ITCZ (Wyrtki, 1973). During boreal winter, ITCZ is located south of equator and shifts to north during boreal summer. This northward shift of ITCZ during southwest monsoon (SWM, June-September) season drives the southern hemisphere eastern trade winds across equator that turn clockwise and becomes southwest winds (Findlater, 1977; Fig. 3). These southwest winds result in Somali current along the east African coast towards north. The Somali current is generally associated with near shore upwelling and eddies such as southern gyre, great whirl and Socotra eddy (Schott et al., 1990; Beal and Chereskin, 2003; Schott et al., 2009). These eddies induce intense upwelling which brings low temperature-nutrient rich subsurface water to the surface along the east coast of Africa (Young and Kindle, 1994).

Productivity in the western Arabian Sea demonstrates seasonal changes in surface ocean characteristics (Qasim, 1977; Brock et al., 1991). More than half of the annual productivity in the western Arabian Sea occurs during southwest monsoon due to intense upwelling (Haake et al., 1993). Total flux (biogenic + dust) peaks during similar period when productivity is at its maximum, indicating that SWM not only results in high productivity in the western Arabian Sea but also contributes to high dust flux (Sirocko and Lange, 1991; Haake et al., 1993). Bhushan et al., 2003 observed that concentration of nitrate and phosphate increased at the bottom of the mixed layer at the core location, whereas significant increase in silicate concentration occurs only at depths of thermocline. During the onset of SWM upwelling, more nitrate and phosphate than silicate reach the surface due to the upwelling of shallow waters. In presence of high nitrate and phosphate along with the micronutrients (derived by dust flux), the calcareous primary producers dominate the surface productivity. Sediment trap studies in the western Arabian Sea recorded high biogenic carbonate flux at the onset of SWM upwelling (Haake et al., 1993). During the late phase of SWM upwelling, the surfacing of deeper waters increased silicate concentration in surface waters. High silicate content and depletion

of micro-nutrients that sustain excessive nutrient utilization results in siliceous productivity and subsequent biogenic silica flux to the sediments (Fig. 1; Koning et al., 2001). Initially, this upwelled deep water surfaced at Somali coastal upwelling zone and was transported towards the mouth of Gulf of Aden (core location) through the Socotra channel i.e. between the Socotra Island and Somalia (Young and Kindle, 1994).

2 Material and methods

A sediment core SS4018 was collected off the Horn of Africa (north of Socotra island), from the western Arabian Sea (13° 12.80' N, 53° 15.40' E; water depth 2830 m; core length 130 cm; Fig. 2) during FORV Sagar Sampada cruise SS-164 in 1998. Sub-sampling of the core was done at 2-cm intervals. The age-depth model (Fig. 4) as well as the calcareous and organic productivity proxies of this sediment core have been presented elsewhere (Tiwari et al., 2010). Dry bulk density (DBD) was computed using an empirical equation based on the calcium carbonate concentrations (Clemens et al., 1987). The flux rate was estimated using an average sedimentation rate computed based on the age-depth model given by Tiwari et al., (2010). The sedimentation rate at the core site as given by Tiwari et al., (2010) is variable, the lowest being 3.5 and highest at 22.7 cm.ka^{-1}. Since the age model depends on the sample selection criteria and may change according to depth of age control points, an average sedimentation rate was computed for the entire core. The actual sedimentation at SS4018 sediment core site is possibly much more complex than the age model presented in Tiwari et al (2010), and thus the average sedimentation rates were computed for the entire core. This average age model is only used to understand large-scale changes in biogenic silica concentration.

The biogenic silica concentration was measured in each sample using the method described by Carter and Colman (1994). Dried homogenized samples weighing 50 mg were placed in centrifuge tubes. Five milliliters of 10 % H_2O_2 was added to each sample at room temperature, and the samples were stored for 2 hours to remove organic matter. Five milliliters of 1N HCl was added to each tube. After acid treatment, sample was washed thoroughly with 20 ml of distilled water, and the samples were centrifuged for 15 minutes. Sample were kept in an oven for drying after removal of the supernatant. Thirty milliliters of 2 M Na_2CO_3 was added to each sample, and were kept in a shaker bath at 95^0 C for 5 hours. After 5 hours, the samples were centrifuged, and 3 ml of hot supernatant was pipetted out of each sample and added to exactly 30 ml of distilled water in pre-cleaned sample tubes. The solution was acidified by adding 0.9 ml of concentrated HNO_3. Sample tubes were sealed after effervescence. The silicon and aluminium concentrations were measured in these samples using ICP-AES (Jobin-Yuvon, Model 38S). The silicon concentrations were then corrected for clay mineral dissolution by using the formula given by Carter and Colman (1994) (Eqn 1):

$$\Delta Si = Si - (Al * 1.93) \quad (1)$$

Where, ΔSi is the corrected silicon concentration, Si and Al are the measured concentrations of silicon and aluminium in the sample, and 1.93 is the Si to Al ratio in smectite. Smectite is an abundant clay mineral in the northern Arabian Sea (Sirocko et al., 1991). Biogenic silica concentrations were calculated using the formula given below (Eqn 2):

$$Biogenic\ silica = \Delta Si * \mathcal{K} \quad (2)$$

Where, K is a constant that equals 2.4, which accounts for the ~10 % water content in biogenic silica (Mortlock and Frolich, 1989). Overall, the error associated with the biogenic silica measurement is less than 5 % based on repeat measurements. The biogenic silica flux is calculated by multiplying the biogenic silica fraction by the sedimentation rate (SR) and the dry bulk density (DBD) (Eqn 3),

$$B.Si.flux(g.m^{-2}.y^{-1}) = B.Si * SR(m.y^{-1}) * DBD(g.m^{-3}) \quad (3)$$

The uncertainties associated with the biogenic silica concentration (B.Si) is estimated from the error in aluminium and silicon concentration based on repeat measurements of standard material. The maximum error in biogenic silica concentration is within 5%. Dry bulk density (DBD) is calculated from CaCO3 concentration using an empirical equation suggested by Clemens et al., 1987. The standard uncertainty in DBD calculation is 0.091 g/cm^3. The uncertainty in average sedimentation rate (SR) is 0.12 cm/ky. The uncertainty associated with biogenic silica flux (B.Si flux) is ~~propagated~~ using the equation below,

$$\sigma B.Si\ flux = B.Si\ flux * \sqrt{\{(\sigma B.Si/_{B.Si})^2 + (\sigma DBD/_{DBD})^2 + (\sigma SR/_{SR})^2\}} \quad (4)$$

Where, prefix "σ" stands for uncertainty. Uncertainty in biogenic silica concentration is below 5%. But the uncertainty in flux are up to 15%. This increase in uncertainty is due to the high standard error associated with empirical derivation of Dry bulk density.

3 Result and Discussion

3.1 Biogenic silica flux vs SST

Similar to biogenic silica flux, the paleo-SST can serve as proxy for upwelling, as upwelling increases siliceous productivity with reduction in SST. However, the inverse relation between siliceous productivity and SST is valid only during the SWM season and not even on annual scale. All SST proxies tend to record annual mean signal with varying fraction of seasonal signal. Glacial boundary conditions have strong influence on the annual mean SST in the Arabian Sea irrespective of monsoon upwelling (Broccoli, 2000; Dahl and Oppo, 2006). However, the biogenic silica flux is controlled by the SWM upwelling after its production during the southwest monsoon season, and therefore preserves the upwelling signal. Hence, the biogenic silica flux can be identified as a better proxy than SST to understand SWM upwelling in the study area. The variations in biogenic silica fluxes during the last 18.5 ka are shown in Fig.5 and the data is presented in Table 1. Comparison of biogenic silica flux with other paleo-SST records (Anand et al., 2008; Sahar et al., 2007; Huguet et al., 2006) from adjacent locations are shown in figure 6 and 8. No definitive relation can be observed between biogenic silica flux and SST records over time. The SST using different proxies show inconsistent changes in the studied time span, the TEX_{86} SST always being higher than Mg/Ca SST (Fig. 6&8). A general observation is that both biogenic silica flux and SST were low during 18.5 to 15 ka BP, later showing an anti-correlation (Fig. 6). The anti-correlation is strong between biogenic silica flux and TEX_{86} SST during 15 to

11.7 ka BP (Fig. 6). However, during the last 11.7 ka the Mg/Ca based SST shows a strong anti-correlation with biogenic silica flux record, indicating variation in the influence of the seasonal signal on different SST proxies (Fig. 8).

3.2 Somali upwelling strength versus southwest monsoon rainfall

The western Arabian Sea SSTs during SWM is directly related to upwelling strength (enhanced upwelling results in lower SSTs and vice versa; Fig. 1). Previous studies have shown the northern Indian ocean and in particular the Arabian Sea to be an important source of moisture for SWM rainfall over India (Ninomiya and Kobayashi, 1999; Gimeno et al., 2010). Various possible relationship are observed between SST, moisture and SWM rainfall. First order relation would be positive, i.e. reduced SWM winds would cause reduced upwelling as well as reduced rainfall and vice versa. However, the relation between Arabian Sea SST and SWM rainfall is complicated due to the fact that SST modulates the moisture availability as well as the meridional temperature gradient (Levine and Turner, 2012). Modelling study by Shukla (1975) showed that the cold Arabian Sea SST during SWM tend to reduce the SWM rainfall through reduced moisture transport. However, Webster et al (1999) and Clark et al (2000) showed that the SWM rainfall has stronger connection with winter and spring SSTs rather than summer, and suggested a delayed influence of SST on rainfall. A modelling study by Arpe et al (1998) demonstrated that warmer northern Indian Ocean leads to increased SWM rainfall over India through enhanced evaporation and moisture supply, while indicating the strong influence of Pacific SST anomalies on monsoon. It was also suggested that Arabian Sea SST modulates the impact of ENSO on monsoon precipitation (Arpe et al., 1998; Lavine and Turner, 2012). An observational study by Vecchi and Harrison (2004) detected a strong positive correlation between western Arabian SSTs and SWM rainfall over the Western Ghats Mountains in India from 1982 to 2001. Overall, it has been suggested that any isolated cooling of the Arabian Sea will reduce SWM rainfall through reduced moisture supply, in absence of other large-scale forcing (Lavine and Turner, 2012). An observational and modelling study by Izumo et al (2008) signals causes for the variations in western Arabian Sea SSTs and its influence on SWM rainfall over the Western Ghats. According to Izumo et al (2008), increased Somali upwelling during the late spring reduces the westward extension of the IOWP during summer, which decreases moisture availability to the air mass delivering rainfall to the western part of the Indian sub-continent. However, the upwelling-rainfall connection is not fully understood and difficult to model, the observations suggest an anti-correlation between Somali upwelling (western Arabian Sea SST during SWM) and SWM rainfall. Both Somali upwelling and SWM rainfall being initiated by the southwest monsoonal winds during SWM season, hence their anti-correlation indicates negative influence of Somali upwelling on SWM rainfall during SWM season.

Did such anti-correlation exist between the Somali upwelling and SWM rainfall in the geological past? To answer this question, we need to investigate the record of paleo-upwelling in the Somali region and paleo-rainfall in the western part of India and adjoining areas. There is no continuous terrestrial record of paleo-rainfall covering the last 18.5 ka from the Western Ghats, but there are several paleoclimatic records based on marine sediment cores from the eastern Arabian Sea. The biogenic silica flux temporal variability is compared (Fig. 7&10) with paleo-rainfall record ($\delta^{18}O_w$IVF by Anand et al., 2008)) from the eastern Arabian Sea and a speleothem record from Oman (Fleitmann et al., 2003). The $\delta^{18}O_w$ IVF is the Ice Volume

Free (IVF) oxygen isotopic composition of seawater based on the $\delta^{18}O$ of *G.ruber*. Anand et al. (2008) showed that the reconstructed $\delta^{18}O_w$ IVF during the last 19 ka from a sediment core (SK-17) in the eastern Arabian Sea was mainly regulated by the SWM rainfall in the Western Ghats. The Qunf speleothem record from Oman (Fleitmann et al., 2003) had been widely used as an indicator for SWM variation. The location of Qunf speleothem is very close to the present study area i.e. downwind side to the present study area during SWM season. If the SWM was the reason for the rainfall in southern Oman, then western Arabian Sea must be the source of moisture. However, there is no observational study on the relation between upwelling strength and rainfall in Oman, but a comparison is made to give a preliminary assessment. Since records are from different regions and have irregular temporal resolution, only long-term trends have been examined.

3.2.1 Last Glacial Period (18.5–15 ka BP)

The biogenic silica flux record does not show any distinct variation between the previously identified Heinrich event 1 and the Last Glacial Maximum (LGM; Clark et al., 2009), the period between 18.5 and 15 ka thus is considered here as the Last Glacial Period (LGP). Both biogenic silica concentrations (3–5 %) and their fluxes (~2 g.m-2.y-1) were lowest during the LGP (Fig. 5), similar to earlier findings of low productivity during glacial periods from the western Arabian Sea (Burckle, 1989; Sirocko et al., 1991; Sirocko et al., 2000; Ivanochko et al., 2005; Tiwari et al., 2010). Based on modern pattern of the biogenic silica productivity and its burial efficiency in the western Arabian Sea, observed low fluxes of biogenic silica indicate that the Somali upwelling was very weak during the LGP. However, the lowest SST recorded in the last 18.5 ka in the Somali basin during the LGP (Huguet et al., 2006; Saher et al., 2007; Anand et al., 2008) is related to basin wide cooling and not connected with upwelling strength (Fig. 6). Dahl and Oppo (2006) observed a reduction in Arabian Sea SST of 2–4° C during LGP. Thus, it is unlikely that the IOWP (SST>28° C) formed during LGP. In absence of IOWP, any relation between the Somali upwelling and rainfall is unexpected. Paleo-rainfall record from the eastern Arabian Sea shows high $\delta^{18}O_w$ IVF values indicative of reduced freshwater flux and rainfall during LGP (Fig. 7). Based on weak upwelling in the western Arabian Sea and reduced fresh water influx to the eastern Arabian Sea, it can be concluded that the SWM was weak/absent during the LGP.

3.2.2 Deglacial Period (15–11.7 ka BP)

The Deglacial Period (DP) is a connecting phase between two entirely different climatic periods, the LGP and the Holocene. The DP basically comprises two millennial scale events between 15–12.9 ka and 12.9–11.7 ka BP. This period nearly coincides with well-known climatic events, specifically the Bølling-Allerød (B/A) and the Younger Dryas (YD) event. The beginning of the B/A is marked by an abrupt increase in biogenic silica flux (Fig. 6a), which is attributed to the effect of northern limit of southwest monsoon, attained at the study site with subsequent increase in Somali upwelling strength. This is further supported by Zr/Hf in two independent sediment cores near study site, which shows an increasing flux of wind borne dust from the Horn of Africa (an indicator of the SWM) at the onset of the B/A (Sirocko et al., 2000; Isaji et al., 2015). The reduction in TEX_{86} SST during the B/A in the Somali basin (Huguet et al., 2006) too suggests increased upwelling (Fig. 5), however the

Mg/Ca SST does not show such variation (Fig. 6). The inconsistency between the two SST records (TEX_{86} and Mg/Ca) can be related to the control on seasonal production of the proxy material.

The $\delta^{18}O_w$IVF record from core SK-17 (Anand et al., 2008) with depleted values~~,~~ indicate higher influx of fresh water from the Western Ghats caused by high SWM rainfall~~,~~ during the B/A (Fig. 7c). The positive correlation between Somali upwelling (high biogenic silica flux) and SWM rainfall in the Western Ghats (high fresh water influx to the eastern Arabian Sea) during the B/A is contrasting with the present-day scenario as observed by Vecchi and Harrison (2004). Presently, the moisture source for the SWM rainfall is the Arabian Sea and the central Indian Ocean (IOWP), which is affected by SWM upwelling (Izumo et al., 2008). If the central Indian Ocean was the source of moisture for SWM rainfall during the B/A, then the observed co-variation is possible. Thus, it is proposed that the moisture source for SWM rainfall over the Western Ghats during the B/A event was different from the modern source. The other possibility of enhanced rainfall in south-western India due to a strong NE monsoon during the B/A is unlikely because the siliceous productivity in the western Arabian Sea related to the NE monsoon has not been reported (Koning et al., 1997; Ramaswamy and Gaye, 2006). In contrast to the B/A, the upwelling in the western Arabian Sea was weak during the YD, as revealed by the low biogenic silica fluxes and high SSTs (Fig. 6; Huguet et al., 2006). This is in agreement with the previous studies from the Arabian Sea which shows decreased productivity during YD due to reduction in SWM (Altabet et al., 2002; Ivanochko et al., 2005). Furthermore, the high $\delta^{18}O_w$IVF in the eastern Arabian Sea (Anand et al., 2008) caused by low freshwater influx points to weak SWM rainfall (Fig.7).

3.2.3 Holocene (11.7–0 ka BP)

The beginning of the Holocene is marked with an abrupt increase in biogenic silica flux (Fig. 8a). This sudden increase in biogenic silica fluxes between 11.7 ka and 9 ka BP could be due to the intensification of the SWM (extended season) resulting from northward shift of the ITCZ, following the peak in Northern Hemisphere solar insolation (Fleitmann et al., 2007). Somali basin SST records (Saher et al., 2007; Huguet et al., 2006; Anand et al., 2008) also show~~s~~ a marginal decrease at the onset of the Holocene, but not to the levels observed during the B/A (Fig.8). The TEX_{86} SST shows more variation than Mg/Ca at the beginning of Holocene, however, the Mg/Ca SST is mirror image of the biogenic silica flux pattern during Holocene, indicating dominance of seasonal signal in Mg/Ca SST during this period (Fig. 8b). Based on the stable isotopic composition of organic carbon and nitrogen in the 4018 core, Tiwari et al (2010) too suggested an increase in productivity during Holocene and attributed it to the strengthening of Somali upwelling. The synchronous changes in the biogenic silica flux with biogenic silica/carbonate ratio (Fig. 9) indicates a change in dominant plankton community (carbonaceous to siliceous) due to increased upwelling, as suggested by Tiwari et al. (2010). The $\delta^{18}O_w$IVF (Anand et al., 2008) display values similar to YD during the early Holocene (Fig. 10c), indicating reduced rainfall (lower fresh water influx) over the Western Ghats. This anti-correlation between Somali upwelling and SWM rainfall over south-western India during the early Holocene (11.7 ka to 9 ka BP)~~,~~ marks the establishment of the modern-day climate system. The increased Somali upwelling in the western Arabian Sea during the early Holocene (11.7 to 8 ka BP; Fig. 10a) could have reduced the IOWP extension during the SWM season, thereby resulting

in lower moisture availability and subsequent reduced rainfall over the Western Ghats. Oman speleothem record also shows decreased precipitation during early Holocene (Fig. 10b) and supports this interpretation of low moisture availability.

At ~8 ka BP (Fig. 10a)~~,~~ compared to the early Holocene, Somali upwelling strength decreased but persisted beyond YD and B/A levels, indicating the presence of SWM with reduced wind strengths relative to the early Holocene. The SST record also shows an increased value at ~8 ka BP (Fig. 8b) indicating reduction in Somali upwelling. This reduction in upwelling at 8 ka BP can support the westward extension of the IOWP during the SWM season, thereby increasing both moisture availability over the Arabian Sea and rainfall over the Western Ghats. The $\delta^{18}O_w$ IVF value decreased at 8 ka BP, indicating an increase in fresh water influx from the Western Ghats (Anand et al., 2008) due to increased SWM rainfall (Fig. 10c). Oman speleothem record too shows decreased $\delta^{18}O$ value at 8 ka BP (Fig. 10b) suggesting increased SWM rainfall.

Somali upwelling had a gradual increase during the last 8 ka with minor positive excursion at around 5 and 2 ka BP (Fig. 10a). The increase in SWM induced Somali upwelling during the last 8 ka contrasts the idea that SWM followed the northern hemisphere insolation during Holocene (Gupta et al., 2003; Fleitmann et al., 2003 and references therein). However, this interpretation is well in agreement with other studies from the Arabian Sea which show~~s~~ that SWM did slightly increase during Holocene (Agnihotri et al., 2003; Tiwari et al., 2010). The short-term increase in Somali upwelling at 5 and 2 ka BP can also be observed with reduction in the Mg/Ca SST record (Fig. 8b). Oman speleothem record shows an increase in $\delta^{18}O$ during the last 8 ka suggesting reduction in SWM rainfall (Fig. 10b). The hiatus in Oman speleothem record at 2 ka BP coincides with the strengthened Somali upwelling (Fig. 10a & b). Strengthened Somali upwelling at 2 ka BP might have reduced the moisture supply for the SWM rainfall over Oman and caused hiatus in the speleothem record. The SK-17 record (Anand et al., 2008) shows slight increase in the $\delta^{18}O_w$IVF of surface waters during the last 8 ka (Fig. 10c) indicating reduction in SWM rainfall. The opposite trend in upwelling and rainfall record during the last 8 ka indicates the negative impact of Somali upwelling on SWM rainfall through changing area of IOWP and moisture availability. However, the short- term variations in upwelling are not observed in the eastern Arabian Sea rainfall record.

It is observed that except at the beginning, the Somali upwelling had a negative impact on southwest monsoon rainfall over south-western India and Oman during Holocene. This finding would have implications in context of the modelling study by deCastro et al. (2016), which shows that Somali upwelling would increase during the twenty-first century.

4 Conclusions

The present study demonstrates the use of biogenic silica flux as a proxy for the temporal variations in the strength of the Somali upwelling during the last 18.5 ka. Some of the salient findings of the present study are summarized below:

1. The Somali upwelling was weak during the LGP coeval with the weak southwest monsoon.
2. The post-glacial onset of the southwest monsoon was marked by an increase in the strength of the Somali upwelling at 15 ka BP, with the eastern Arabian Sea records showing increased southwest monsoon rainfall.

3. The Somali upwelling was weak between 12.9 and 11.7 ka BP, indicating another phase of weak southwest monsoon like that of the LGP. Overall, records of the Somali upwelling and southwest monsoon rainfall exhibit positive correlations between 18.5 and 11.7 ka BP.
4. A shift from positive to negative correlation between the Somali upwelling strength and southwest monsoon rainfall occurred at 11.7 ka BP at the beginning of the Holocene, which marks the establishment of modern day climate system.
5. Enhanced Somali upwelling during the last 11.7 ka BP, except for a decline at 8 ka BP, had a negative impact on southwest monsoon rainfall.

Acknowledgments

Balaji D. is thankful to the Council of Scientific and Industrial Research (CSIR) of India for providing support through a CSIR-NET-Senior Research Fellowship. Ravi Bhushan thanks Director of the PRL for research grant support. We thank Dr. Alpa Sridhar for critical comments and suggestions on the manuscript. We thank Professor Eduardo Zorita (editor) and three anonymous reviewers for their constructive comments which helped in improving the manuscript.

References

Agnihotri R, Bhattacharya SK, Sarin MM, Somayajulu BLK.: Changes in the surface productivity and subsurface denitrification during the Holocene: a multiproxy study from the eastern Arabian Sea. The Holocene 13: 701–713, 2003.

Altabet, M. A., Higginson, M. J., & Murray, D. W.: The effect of millennial-scale changes in Arabian Sea denitrification on atmospheric CO 2. Nature, 415(6868), 159, 2002.

Anand, P., Kroon, D., Singh, A. D., Ganeshram, R. S., Ganssen, G., and Elderfield, H.: Coupled sea surface temperature–seawater $\delta^{18}O$ reconstructions in the Arabian Sea at the millennial scale for the last 35 ka, Paleoceanography, 23, 2008.

Annamalai, H., and Liu, P.: Response of the Asian summer monsoon to changes in El Nino properties, Quarterly Journal of the Royal Meteorological Society, 131, 805-831, 2005.

Arpe K, Du¨menil L, Giorgetta MA.: Variability of the Indian monsoon in the ECHAM3 model: sensitivity to sea surface temperature, soil moisture, and the stratospheric quasi-biennial oscillation. J Clim 11:1837–1858, 1998.

Beal, L. M., and Chereskin, T. K.: The volume transport of the Somali Current during the 1995 southwest monsoon, Deep Sea Research Part II: Topical Studies in Oceanography, 50, 2077-2089, 2003.

Berrisford, P., Kållberg, P., Kobayashi, S., Dee, D., Uppala, S., Simmons, A., Poli, P., and Sato, H.: Atmospheric conservation properties in ERA-Interim, Quarterly Journal of the Royal Meteorological Society, 137, 1381-1399, 2011.

Bhushan, R., Dutta, K., Mulsow, S., Povinec, P. P., & Somayajulu, B. L. K.: Distribution of natural and man-made radionuclides during the reoccupation of GEOSECS stations 413 and 416 in the Arabian Sea: temporal changes. Deep Sea Research Part II: Topical Studies in Oceanography, 50(17-21), 2777-2784, 2003.

Brassell, S. C., G. Eglinton, I. T. Marlowe, U. Pflaumann, and M. Sarnthein.: Molecular stratigraphy: A new tool for climatic assessment, Nature, 320, 129– 133, 1986.

Broccoli, A. J.: Tropical cooling at the Last Glacial Maximum: An atmosphere–mixed layer ocean model simulation. Journal of Climate, 13(5), 951-976, 2000.

Burckle, L. H.: Distribution of diatoms in sediments of the northern Indian Ocean: Relationship to physical oceanography, Marine Micropaleontology, 15, 53-65, 1989.

Carter, S. J., and Colman, S. M.: Biogenic silica in Lake Baikal sediments: results from 1990–1992 American cores, Journal of Great Lakes Research, 20, 751-760, 1994.

Chave, K. E.: Aspects of the biogeochemistry of magnesium. 1. Calcareous marine organisms, J. Geol., 62, 266–283, 1954.

Clark CO, Cole JE, Webster PJ.: Indian Ocean SST and Indian Summer Rainfall: predictive relationships and their decadal variability. J Clim 13:2503–2519, 2000.

Clark, P.U., Dyke, A.S., Shakun, J.D., Carlson, A.E., Clark, J., Wohlfarth, B., Mitrovica, J.X., Hostetler, S.W. and McCabe, A.M.: The last glacial maximum. Science, 325(5941), pp.710-714, 2009.

Clemens, S. C., Prell, W. L., and Howard, W. R.: Retrospective dry bulk density estimates from southeast Indian Ocean sediments—comparison of water loss and chloride-ion methods, Marine geology, 76, 57-69, 1987.

Conan, S. H., &Brummer, G. J. A.: Fluxes of planktic foraminifera in response to monsoonal upwelling on the Somalia Basin margin. Deep Sea Research Part II: Topical Studies in Oceanography, 47(9-11), 2207-2227, 2000.

Dahl, K. A., and Oppo, D. W.: Sea surface temperature pattern reconstructions in the Arabian Sea, Paleoceanography, 21, 2006.

Emiliani, C.: Pleistocene temperatures, J. Geol, 63, 538– 578, 1955.

Findlater, J.: Observational aspects of the low-level cross-equatorial jet stream of the western Indian Ocean, in: Monsoon Dynamics, Springer, 1251-1262, 1978.

Fleitmann, D., Burns, S. J., Mudelsee, M., Neff, U., Kramers, J., Mangini, A., & Matter, A.: Holocene forcing of the Indian monsoon recorded in a stalagmite from southern Oman. Science, 300(5626), 1737-1739, 2003.

Fleitmann, D., Burns, S. J., Mangini, A., Mudelsee, M., Kramers, J., Villa, I., Neff, U., Al-Subbary, A. A., Buettner, A., and Hippler, D.: Holocene ITCZ and Indian monsoon dynamics recorded in stalagmites from Oman and Yemen (Socotra), Quaternary Science Reviews, 26, 170-188, 2007.

Gimeno L, Drumond A, Nieto R, Trigo RM, Stohl A.: On the origin of continental precipitation. Geophys Res Lett 37:L13804, 2010.

Goswami, B., Krishnamurthy, V., and Annmalai, H.: A broad-scale circulation index for the interannual variability of the Indian summer monsoon, Quarterly Journal of the Royal Meteorological Society, 125, 611-633, 1999.

Goswami, B., Madhusoodanan, M., Neema, C., and Sengupta, D.: A physical mechanism for North Atlantic SST influence on the Indian summer monsoon, Geophysical Research Letters, 33, 2006.

Govil, P., and Naidu, P. D.: Evaporation-precipitation changes in the eastern Arabian Sea for the last 68 ka: Implications on monsoon variability, Paleoceanography, 25, 2010.

Gupta, A. K., Anderson, D. M., and Overpeck, J. T.: Abrupt changes in the Asian southwest monsoon during the Holocene and their links to the North Atlantic Ocean, Nature, 421, 354-357, 2003.

Haake, B., Ittekkot, V., Rixen, T., Ramaswamy, V., Nair, R., and Curry, W.: Seasonality and interannual variability of particle fluxes to the deep Arabian Sea, Deep Sea Research Part I: Oceanographic Research Papers, 40, 1323-1344, 1993.

Hahn, D. G., and Shukla, J.: An apparent relationship between Eurasian snow cover and Indian monsoon rainfall, Journal of the Atmospheric Sciences, 33, 2461-2462, 1976.

Hertzberg, J. E., Schmidt, M. W., Bianchi, T. S., Smith, R. W., Shields, M. R., &Marcantonio, F.: Comparison of eastern tropical Pacific TEX 86 and Globigerinoides ruber Mg/Ca derived sea surface temperatures: Insights from the Holocene and Last Glacial Maximum. Earth and Planetary Science Letters, 434, 320-332, 2016.

Huguet, C., Kim, J. H., SinninghеDamsté, J. S., and Schouten, S.: Reconstruction of sea surface temperature variations in the Arabian Sea over the last 23 kyr using organic proxies (TEX_{86} and $U_{37}K'$), Paleoceanography, 21, 2006.

Hurd, D. C.: Interactions of biogenic opal, sediment and seawater in the Central Equatorial Pacific, Geochimicaetcosmochimicaacta, 37, 2257IN12267-22662282, 1973.

Isaji, Y., Kawahata, H., Ohkouchi, N., Ogawa, N. O., Murayama, M., Inoue, K., and Tamaki, K.: Varying responses to Indian monsoons during the past 220 kyr recorded in deep-sea sediments in inner and outer regions of the Gulf of Aden, Journal of Geophysical Research: Oceans, 120, 7253-7270, 2015.

Ivanochko, T. S., Ganeshram, R. S., Brummer, G.-J. A., Ganssen, G., Jung, S. J., Moreton, S. G., and Kroon, D.: Variations in tropical convection as an amplifier of global climate change at the millennial scale, Earth and Planetary Science Letters, 235, 302-314, 2005.

Izumo, T., Montégut, C. B., Luo, J.-J., Behera, S. K., Masson, S., and Yamagata, T.: The role of the western Arabian Sea upwelling in Indian monsoon rainfall variability, Journal of Climate, 21, 5603-5623, 2008.

Kim, J.-H., Schouten, S., Hopmans, E., Donner, B., SinninghеDamsté, J.S.: Global sediment core-top calibration of the TEX86paleothermometer in the ocean. Geochim. Cosmochim. Acta72, 1154–1173, 2008.

Kim, J.-H., van der Meer, J., Schouten, S., Helmke, P., Willmott, V., Sangiorgi, F., Koc, N., Hopmans, E., SinninghеDamsté, J.S.: New indices and calibrations derived from the distribution of crenarchaealisoprenoidtetraether lipids: impli-cations for past sea surface temperature reconstructions. Geochim. Cosmochim. Acta74, 4639–4654, 2010.

Koning, E., Brummer, G.-J., Van Raaphorst, W., Van Bennekom, J., Helder, W., and Van Iperen, J.: Settling, dissolution and burial of biogenic silica in the sediments off Somalia (northwestern Indian Ocean), Deep Sea Research Part II: Topical Studies in Oceanography, 44, 1341-1360, 1997.

Koning, E., Van Iperen, J., Van Raaphorst, W., Helder, W., Brummer, G.-J., and Van Weering, T.: Selective preservation of upwelling-indicating diatoms in sediments off Somalia, NW Indian Ocean, Deep Sea Research Part I: Oceanographic Research Papers, 48, 2473-2495, 2001.

Krishnamurthy, L., and Krishnamurthy, V.: Teleconnections of Indian monsoon rainfall with AMO and Atlantic tripole, Climate Dynamics, 46, 2269-2285, 2016.

Krishnan, R., and Sugi, M.: Pacific decadal oscillation and variability of the Indian summer monsoon rainfall, Climate Dynamics, 21, 233-242, 2003.

Lea, D. W.: Elemental and isotopic proxies of past ocean temperatures, in Treatise on Geochemistry, vol. 6, The Ocean and Marine Geochemistry, edited by H. D. Holland and K. K. Turekian, pp. 365–390, Elsevier, New York, 2003.

Lee, K.-E., Kim, J.-H., Wilke, I., Helmke, P., Schouten, S.: A study of the alkenone, TEX86, and planktonic foraminifera in the Benguela Upwelling Sys-tem: implications for past sea surface temperature estimates. Geochem. Geo-phys. Geosyst.9, Q10019, 2008.

Levine RC, Turner AG.: Dependence of Indian monsoon rainfall on moisture fluxes across the Arabian Sea and the impact of coupled model sea surface temperature biases. ClimDyn 38:2167–2190, 2012.

Lopes dos Santos, R., Prange, M., Castañeda, I.S., Schefuß, E., Mulitza, S., Schulz, M., Niedermeyer, E.M., SinninghеSamsté, J.S., Schouten, S.: Glacial-interglacial variability in Atlantic meridional overturning circulation and thermocline ad-justments in the tropical North Atlantic. Earth Planet. Sci. Lett.300, 407–414, 2010.

M., d., Sousa, M., Santos, F., Dias, J., and Gómez-Gesteira, M.: How will Somali coastal upwelling evolve under future warming scenarios?, Scientific Reports, 6, 2016.

Mooley, D., Parthasarathy, B., and Pant, G.: Relationship between Indian Summer Monsoon Rainfall and Location of the Ridge at the 500-mb Level along 75° E, Journal of climate and applied meteorology, 25, 633-640, 1986.

Mortlock, R. A., and Froelich, P. N.: A simple method for the rapid determination of biogenic opal in pelagic marine sediments, Deep Sea Research Part A. Oceanographic Research Papers, 36, 1415-1426, 1989.

Naidu, P. D., and Malmgren, B. A.: A high-resolution record of late Quaternary upwelling along the Oman Margin, Arabian Sea based on planktonic foraminifera, Paleoceanography, 11, 129-140, 1996.

Ninomiya, K., and Kobayashi, C.: Precipitation and Moisture Balance of the Asian Summer Monsoon in 1991, Journal of the Meteorological Society of Japan. Ser. II, 77, 77-99, 1999.

Pant, G. B., and Kumar, K. R.: Climates of south Asia, John Wiley & Sons, 1997.

Parthasarathy, B., Diaz, H., and Eischeid, J.: Prediction of all-India summer monsoon rainfall with regional and large-scale parameters, Journal of Geophysical Research: Atmospheres, 93, 5341-5350, 1988.

Parthasarathy, B., Kumar, K. R., and Munot, A.: Evidence of secular variations in Indian monsoon rainfall–circulation relationships, Journal of Climate, 4, 927-938, 1991.

Prahl, F.G., Wakeham, S.G.: Calibration of unsaturation patterns in long-chain ketone compositions for paleotemperature assessment. Nature330, 367–369, 1987.

Qasim, S.: Biological productivity of the Indian Ocean, Indian Journal of Marine Sciences, 6, 16, 1977.

R., S.: Ocean Data View, 2016.

Ramaswamy, V., and Gaye, B.: Regional variations in the fluxes of foraminifera carbonate, coccolithophorid carbonate and biogenic opal in the northern Indian Ocean, Deep Sea Research Part I: Oceanographic Research Papers, 53, 271-293, 2006.

Saher, M., Jung, S., Elderfield, H., Greaves, M., and Kroon, D.: Sea surface temperatures of the western Arabian Sea during the last deglaciation, Paleoceanography, 22, 2007.

Schott, F., Swallow, J. C., and Fieux, M.: The Somali Current at the equator: annual cycle of currents and transports in the upper 1000 m and connection to neighbouring latitudes, Deep Sea Research Part A. Oceanographic Research Papers, 37, 1825-1848, 1990.

Schott, F. A., Xie, S. P., and McCreary, J. P.: Indian Ocean circulation and climate variability, Reviews of Geophysics, 47, 2009.

Schouten, S., E. C. Hopmans, E. Schefuss, and J. S. SinninghеDamste´.: Distributional variations in marine crenarchaeotal membrane lipids: A new tool for reconstructing ancient sea water temperatures?, Earth Planet. Sci. Lett., 204, 265– 274, 2002.

Seki, O., Schmidt, D., Schouten, S., Hopmans, E., SinninghеDamsté, J., Pancost, R.: Paleoceanographic changes in the eastern Equatorial Pacific over the last 10 Myr. Paleoceanography27, PA3224, 2012.

Shukla J.: Effect of Arabian Sea-surface temperature anomaly on Indian summer monsoon: a numerical experiment with the GFDL model. J AtmosSci 32(3):503–511, 1975.

Sirocko, F., and Lange, H.: Clay-mineral accumulation rates in the Arabian Sea during the late Quaternary, Marine Geology, 97, 105-119, 1991.

Sirocko, F., Sarnthein, M., Lange, H., and Erlenkeuser, H.: Atmospheric summer circulation and coastal upwelling in the Arabian Sea during the Holocene and the last glaciation, Quaternary Research, 36, 72-93, 1991.

Sirocko, F., Sarnthein, M., Erlenkeuser, H., Lange, H., Arnold, M., and Duplessy, J.: Century-scale events in monsoonal climate over the past 24,000 years, Nature, 364, 322-324, 1993.

Sirocko, F., Garbe-Schönberg, D., and Devey, C.: Processes controlling trace element geochemistry of Arabian Sea sediments during the last 25,000 years, Global and Planetary Change, 26, 217-303, 2000.

Tiwari, M., Ramesh, R., Bhushan, R., Sheshshayee, M. S., Somayajulu, B. L., Jull, A., and Burr, G. S.: Did the Indo-Asian summer monsoon decrease during the Holocene following insolation?, Journal of Quaternary Science, 25, 1179-1188, 2010.

Vecchi, G. A., and Harrison, D.: Interannual Indian rainfall variability and Indian Ocean sea surface temperature anomalies.. In Earth Climate: The Ocean-Atmosphere Interaction, C. Wang, S. P. Xie& J.A. Carton (eds.), American Geophysical Union., Geophysical Monograph, 147, 247-259, 2004.

Webster PJ, Moore AM, Loschnigg JP, Leben RR.: Coupled ocean–atmosphere dynamics in the Indian Ocean during 1997–98. Nature 401:356–360, 1999.

Wuchter, C., Schouten, S., Wakeham, S.G., SinninghеDamsté, J.S.:Archaealtetraether membrane lipid fluxes in the northeastern Pacific and the Arabian Sea: implications for TEX86paleothermometry. Paleoceanography21, PA4208, 2006.

Wyrtki, K.: Physical oceanography of the Indian Ocean, in: The biology of the Indian Ocean, Springer, 18-36, 1973.

Yadav, R. K.: On the relationship between east equatorial Atlantic SST and ISM through Eurasian wave, Climate Dynamics, 48, 281-295, 2017.

Young, D. K., and Kindle, J. C.: Physical processes affecting availability of dissolved silicate for diatom production in the Arabian Sea, Journal of Geophysical Research: Oceans, 99, 22619-22632, 1994.

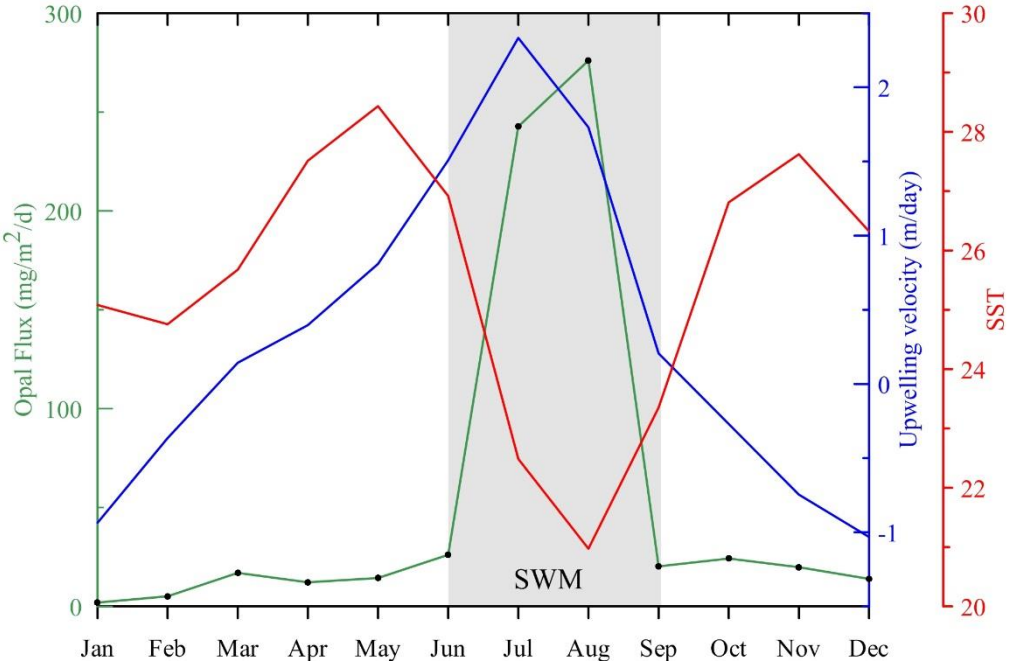

Figure 1. Modern oceanography of western Arabian Sea. Synchronous change in upwelling intensity and biogenic silica flux clearly indicate that the siliceous productivity in western Arabian Sea is controlled by SWM upwelling. Upwelling strength data is used from Nair, 2000 and Opal flux from Haake et al., 2003.

475

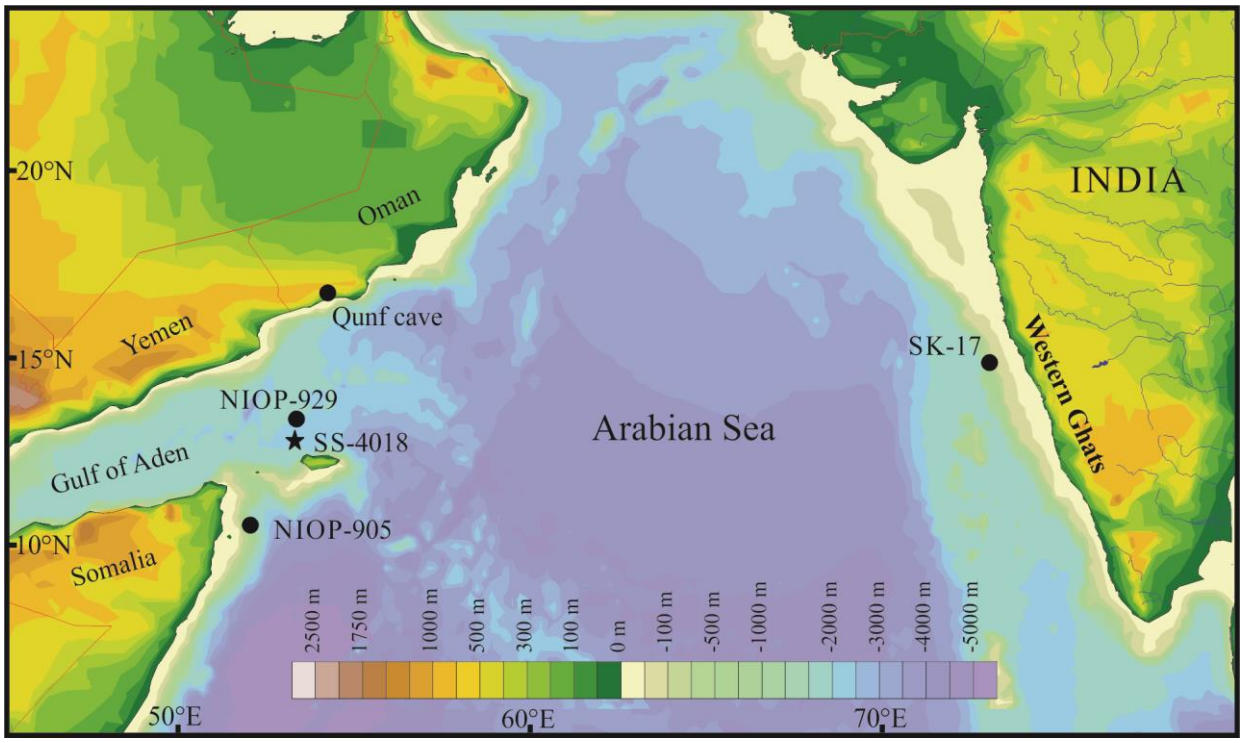

Figure 2: Location of sediment core SS-4018 (filled star) in the Arabian Sea. Also shown are the sites discussed in the paper: NIOP-929 (Saher et al., 2007), NIOP-905 (Huguet et al., 2006), SK-17 (Anand et al., 2008), Qunf cave (Fleitmann et al., 2007).

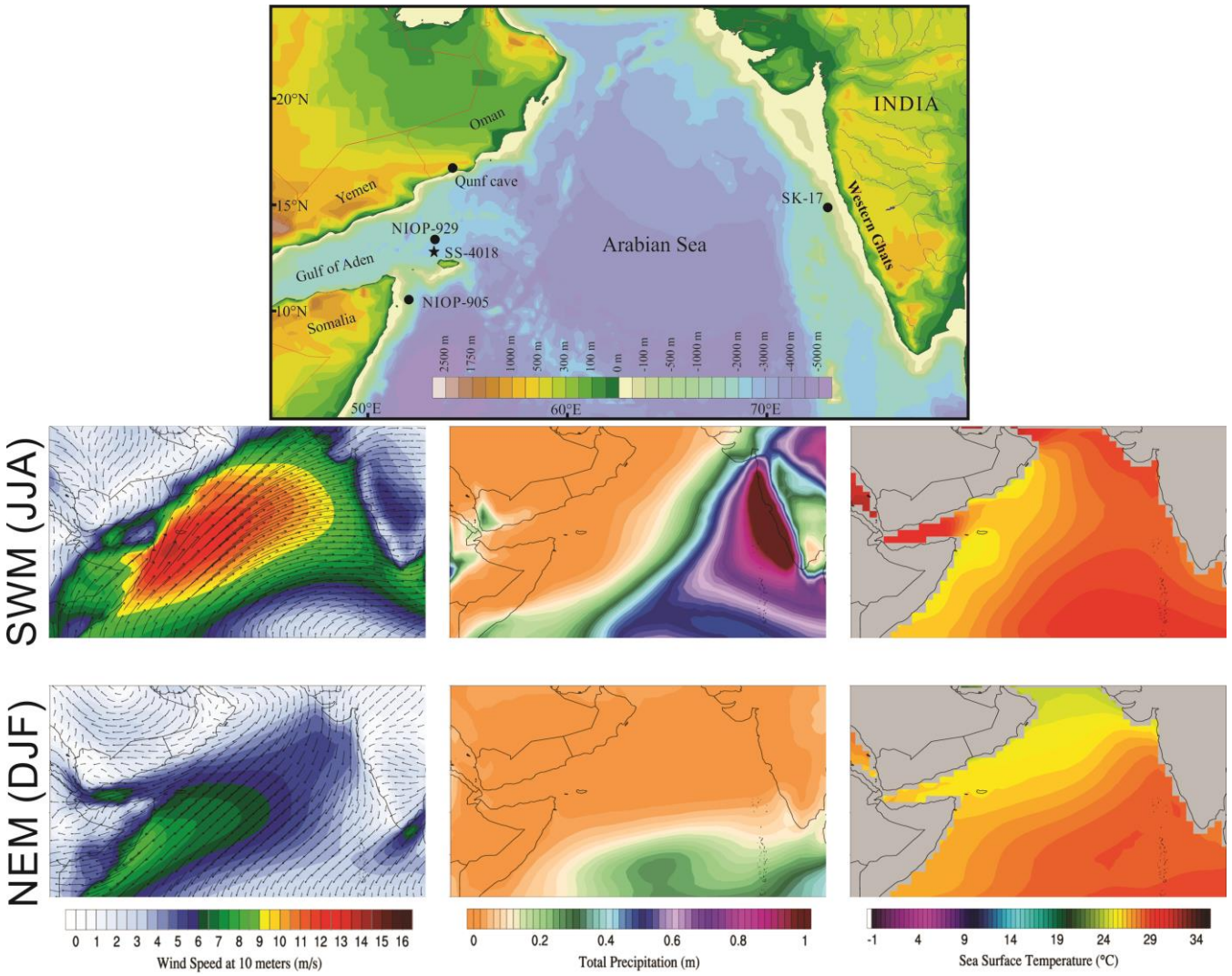

Figure 3: Location of sediment core SS4018 in the western Arabian Sea. Also shown are the sites discussed in the manuscript. Bottom figures shows the seasonal changes in Wind speed, Precipitation and SST during southwest (SWM) and northeast monsoon (NEM). ECMWF-ERA-Interim data (Berrisford et al., 2011) used and the image obtained using Climate Reanalyzer (http://cci-reanalyzer.org), Climate Change Institute, University of Maine, USA.

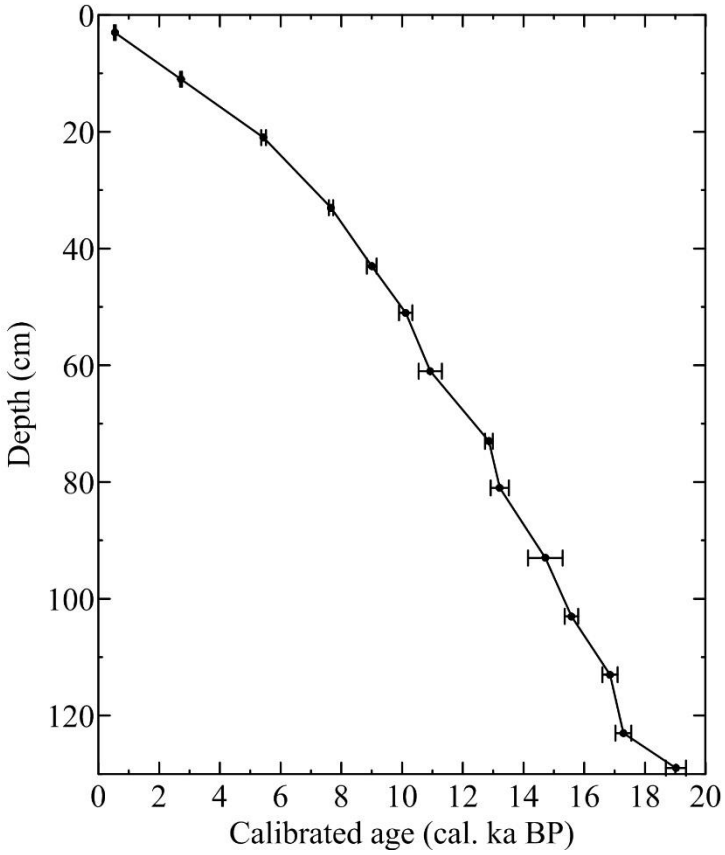

485

Figure 4: Age depth model of the sediment core SS-4018 (adopted from Tiwari et al., 2010). The error bars marks one sigma uncertainty in calibrated age.

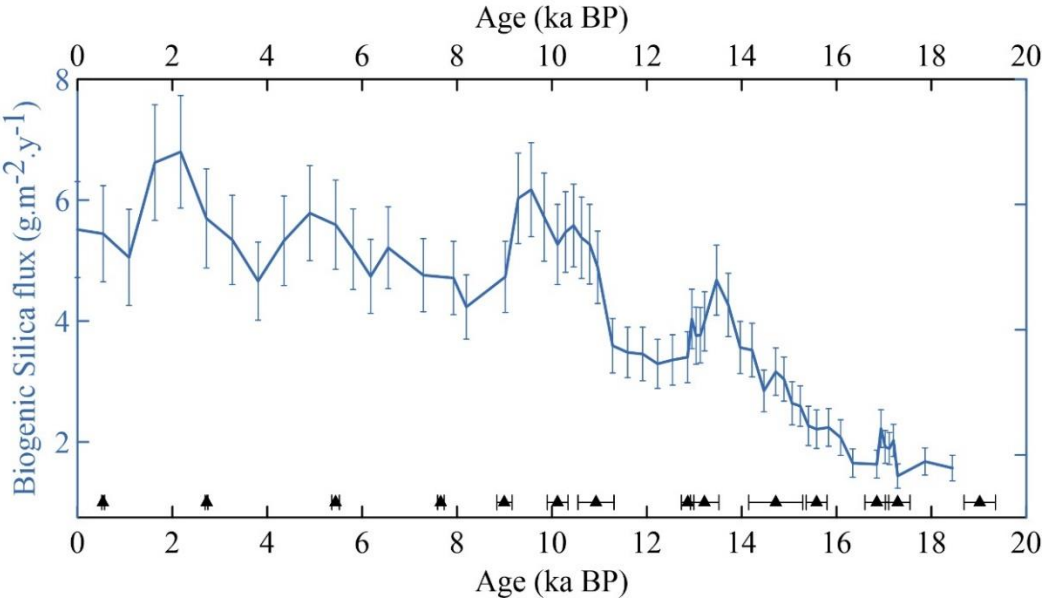

Figure 5: Temporal variation of Biogenic silica flux with two sigma uncertainty in sediment core SS4018. Filled triangles at the bottom of the plot marks the age-control points with one sigma uncertainty.

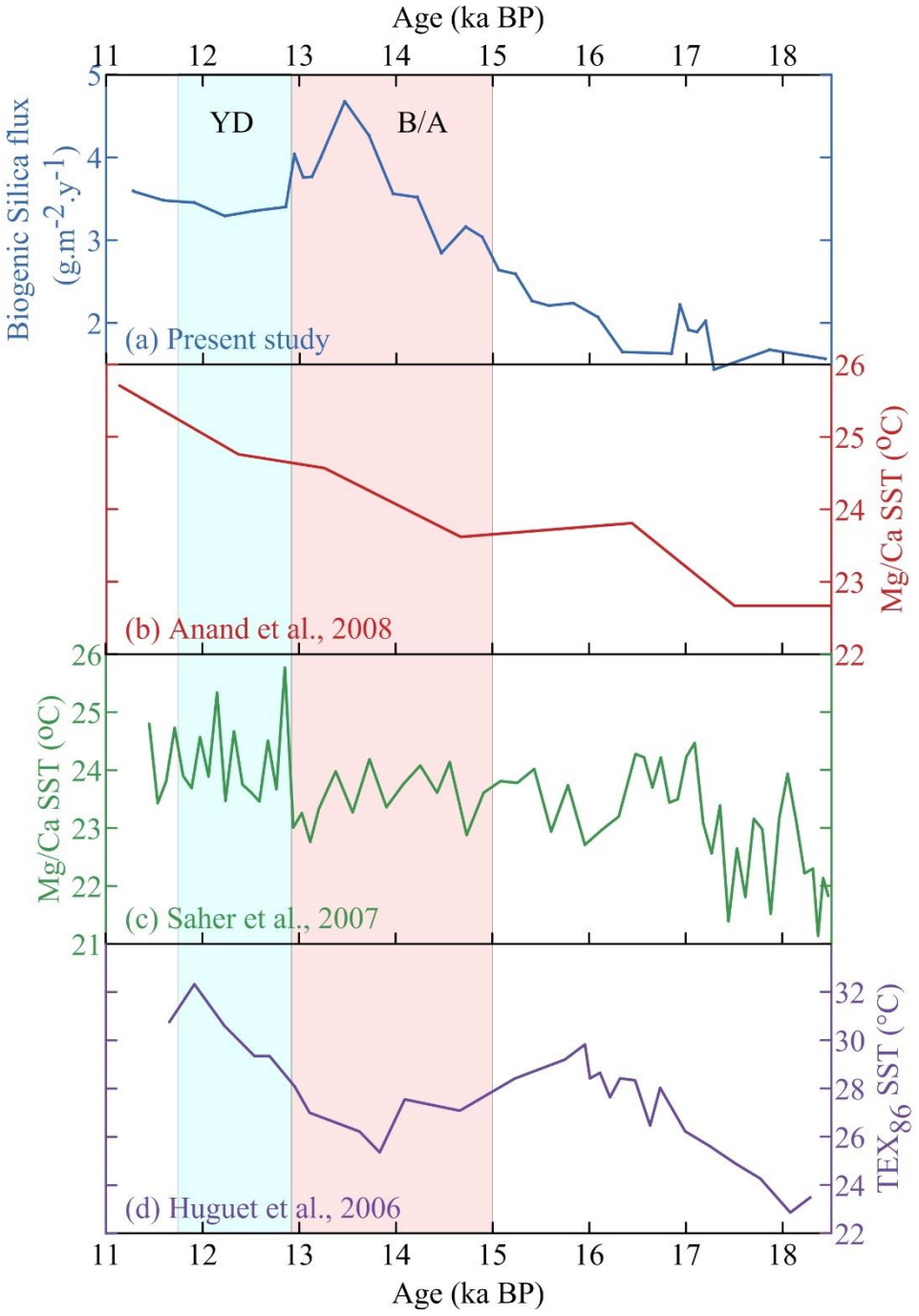

Figure 6. Comparison of biogenic silica flux with SST records from western Arabian Sea for pre-Holocene time (18.5-11.7 ka BP). a)Biogenic silica flux, b) Mg/Ca based SST from NIOP-905 core (Anand et al., 2008), c) Mg/Ca based SST from NIOP-929 core (Saher et al., 2007), d) TEX_{86} SST from NIOP-905 core (Huguet et al., 2006).

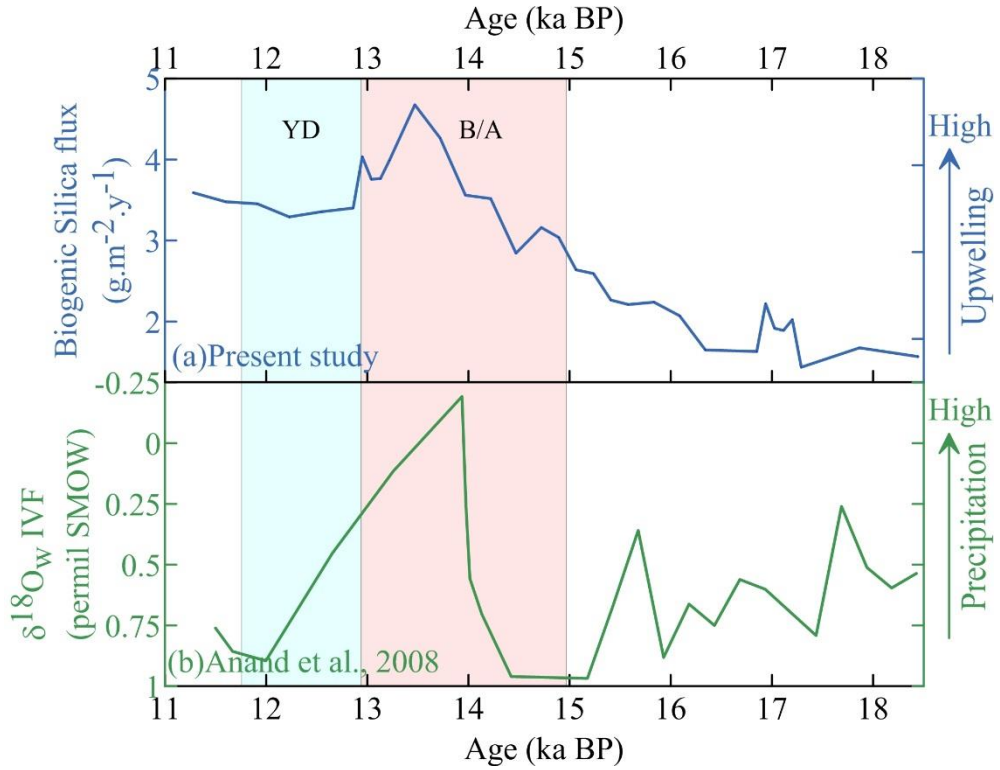

Figure 7. Comparison of biogenic silica flux with rainfall record from eastern Arabian Sea for pre-Holocene time (18.5-11.7 ka BP). (a) Biogenic silica flux (present study), (b) $\delta^{18}O_w$ IVF (Anand et al., 2008).

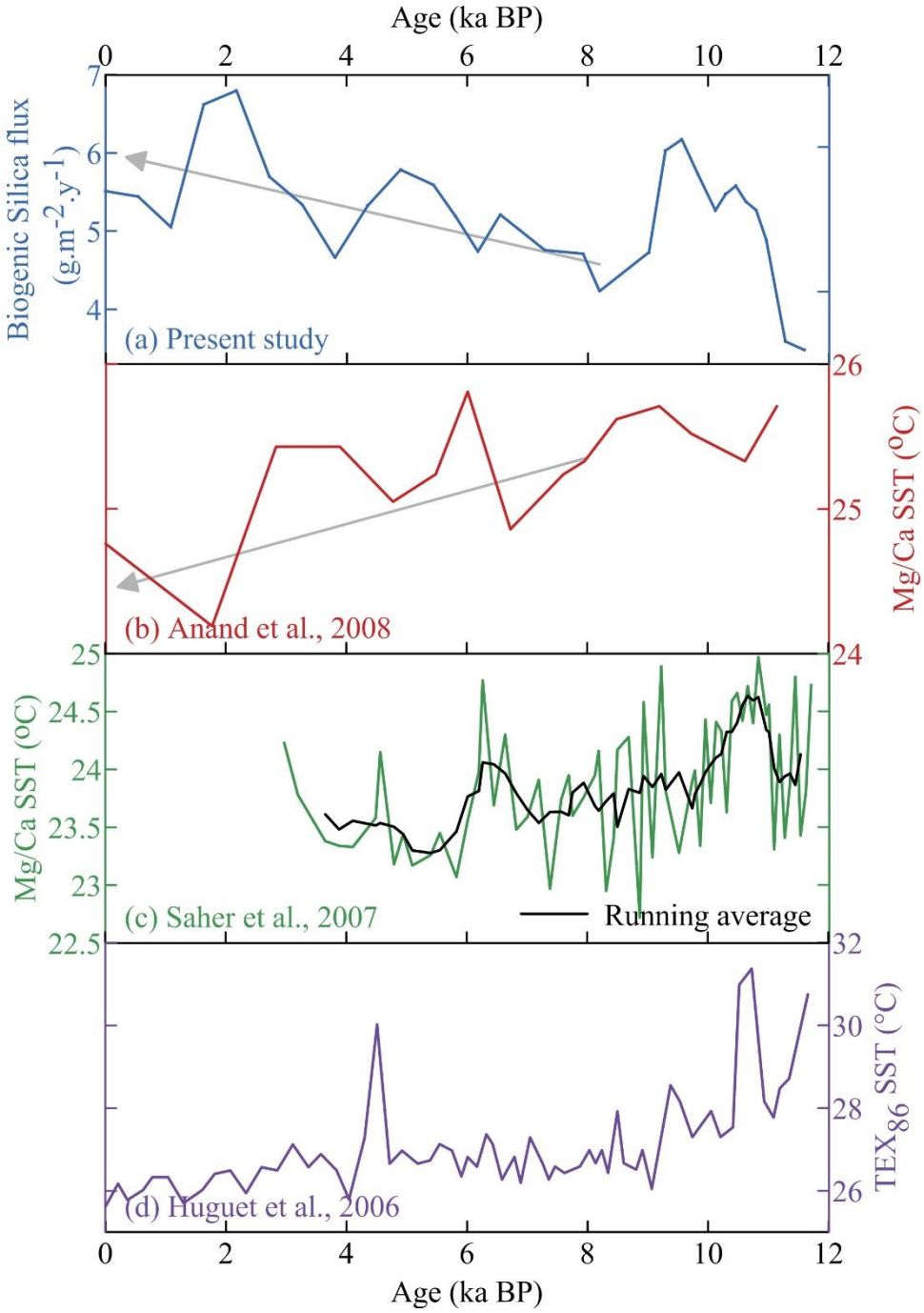

500

Figure 8: Comparison of Somali upwelling with western Arabian Sea SST records. a) Biogenic silica flux, b) Mg/Ca based SST from NIOP-905 core (Anand et al., 2008), c) Mg/Ca based SST from NIOP-929 core (Saher et al., 2007), d) TEX_{86} SST from NIOP-905 core (Huguet et al., 2006). Grey arrow indicate the trend of proxy records during the last 8 ka.

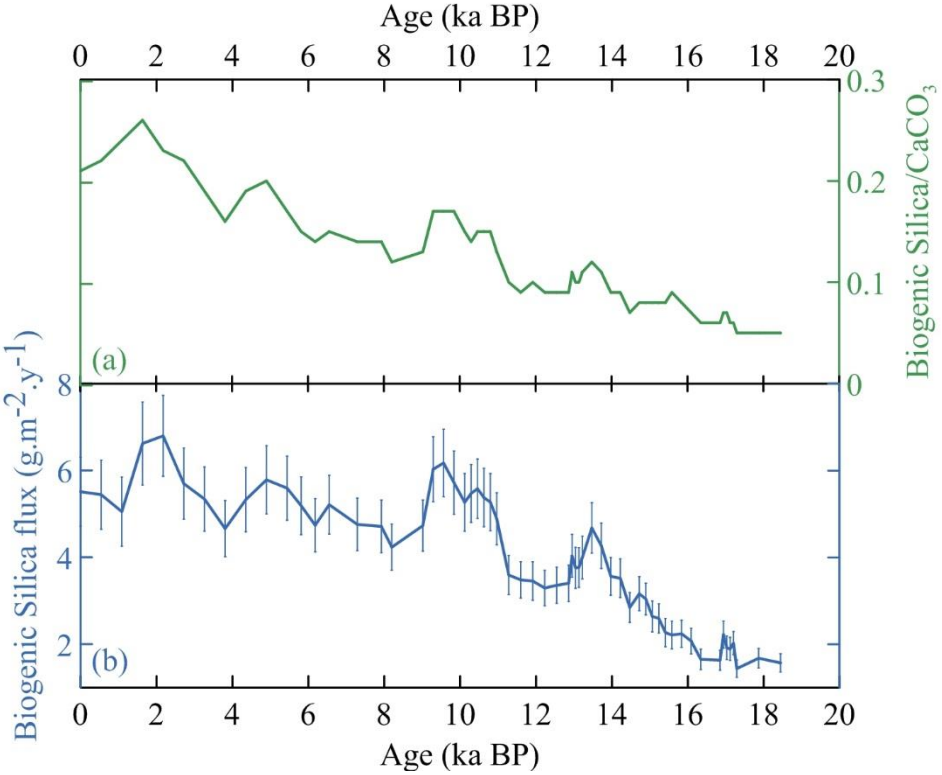

505

Figure 9: Comparison of biogenic silica flux with silica to carbonate ratio in 4018 sediment core. Synchronous changes in both parameters indicate the dominance of biogenic silica flux on the ratio.

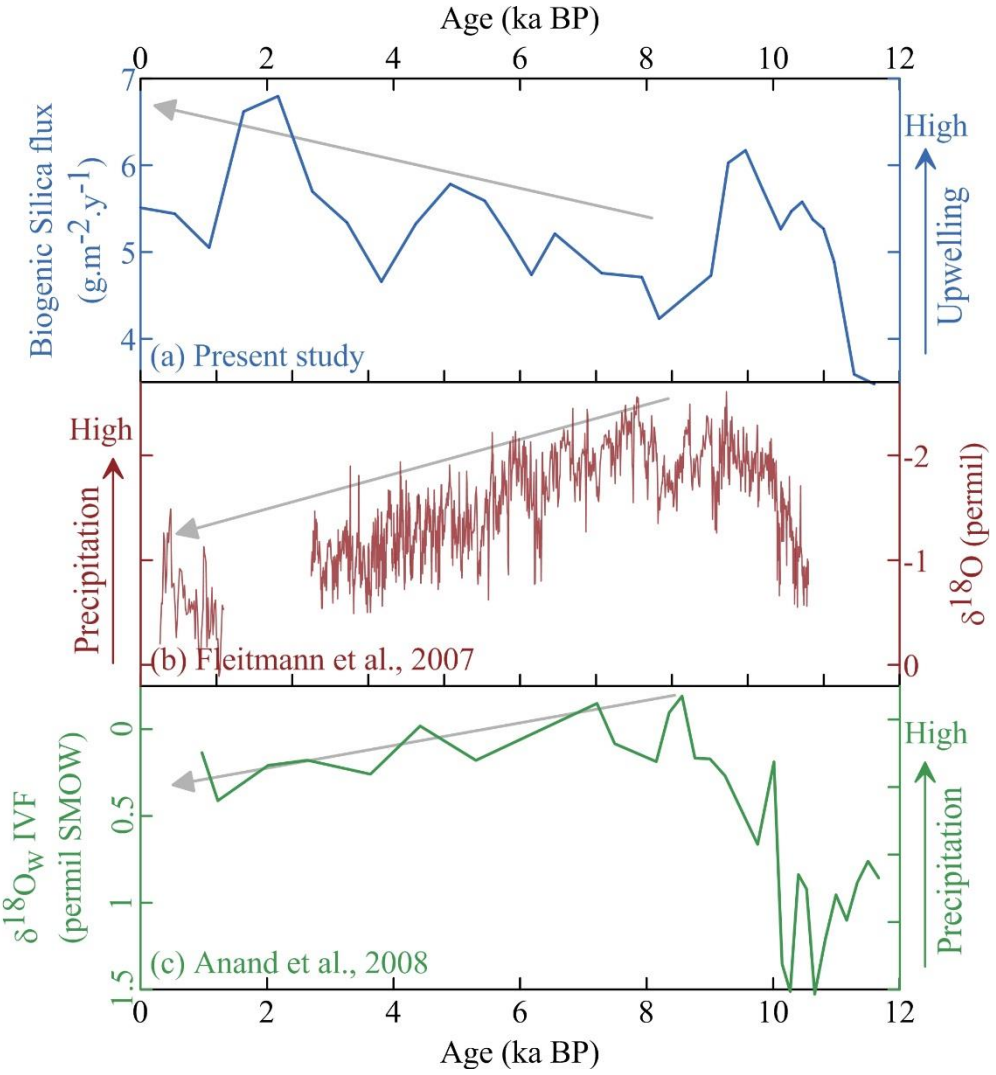

Figure 10: Comparison of Somali upwelling with southwest monsoon rainfall records during Holocene. (a) Biogenic silica flux (present study), (b) Oman speleothem record, (c) $\delta^{18}O_w$IVF data from eastern Arabian Sea. Grey arrow indicate the trend of proxy record during the last 8 ka.

Age (ky)	B. Si (%)	σ B.Si	B.Si flux ($g/m^2/y$)	σB.Si flux	Age (ky)	B. Si (%)	σ B.Si	B.Si flux ($g/m^2/y$)	σB.Si flux
0.00	12.58	0.22	5.51	0.79	12.23	6.41	0.11	3.29	0.41
0.54	12.58	0.25	5.44	0.80	12.54	6.49	0.16	3.36	0.42
1.09	12.58	0.28	5.05	0.80	12.86	6.49	0.20	3.40	0.42
1.63	15.20	0.20	6.62	0.96	12.95	7.76	0.13	4.03	0.49
2.17	14.81	0.14	6.80	0.93	13.04	7.37	0.18	3.76	0.47
2.72	13.06	0.05	5.70	0.82	13.13	7.24	0.09	3.77	0.46
3.26	11.70	0.21	5.34	0.74	13.22	7.74	0.13	3.99	0.49
3.81	10.23	0.17	4.66	0.65	13.47	9.06	0.21	4.68	0.58
4.35	11.79	0.10	5.33	0.74	13.72	8.23	0.16	4.27	0.52
4.90	12.49	0.13	5.78	0.79	13.97	6.83	0.11	3.56	0.43
5.44	11.64	0.22	5.59	0.74	14.22	6.83	0.22	3.52	0.44
5.81	10.52	0.17	5.19	0.67	14.47	5.41	0.10	2.84	0.34
6.18	9.74	0.04	4.74	0.61	14.72	6.11	0.16	3.16	0.39
6.55	10.52	0.29	5.21	0.68	14.89	5.74	0.09	3.04	0.36
7.29	9.59	0.12	4.76	0.61	15.06	5.49	0.19	2.64	0.36
7.93	9.59	0.15	4.71	0.61	15.24	5.24	0.14	2.59	0.34
8.20	8.31	0.19	4.23	0.53	15.41	5.07	0.15	2.27	0.32
9.02	9.35	0.10	4.73	0.59	15.58	5.08	0.04	2.21	0.32
9.29	11.88	0.09	6.03	0.75	15.83	4.94	0.08	2.24	0.31
9.56	12.28	0.19	6.17	0.78	16.09	4.53	0.17	2.07	0.29
9.84	11.57	0.14	5.72	0.73	16.34	3.66	0.11	1.65	0.23
10.12	10.43	0.21	5.26	0.66	16.85	3.54	0.13	1.63	0.23
10.29	10.57	0.10	5.47	0.67	16.94	4.75	0.20	2.22	0.31
10.46	10.82	0.14	5.58	0.68	17.03	4.17	0.15	1.92	0.27
10.63	10.59	0.20	5.38	0.67	17.11	4.04	0.17	1.89	0.27
10.80	10.45	0.11	5.27	0.66	17.20	4.17	0.08	2.02	0.26
10.97	9.47	0.12	4.89	0.60	17.29	3.05	0.12	1.44	0.20
11.28	7.04	0.17	3.59	0.45	17.87	3.52	0.09	1.68	0.22
11.60	6.59	0.09	3.48	0.42	18.44	3.25	0.11	1.57	0.21
11.91	6.92	0.17	3.45	0.44					

Table 1: Biogenic silica concentration and flux data.